PNAS Nexus, 2024, 3, pgae234
https://doi.org/10.1093/pnasnexus/pgae234
Advance access publication 12 June 2024
Research Report

A leak K^+ channel TWK-40 sustains the rhythmic motor program

Zhongpu Yue[a,1], Yi Li[a,1], Bin Yu[a,1], Yueqing Xu[b,1], Lili Chen[a], Jyothsna Chitturi[c], Jun Meng[c], Ying Wang[c], Yuhang Tian[d], Sonia El Mouridi[e,f], Cuntai Zhang[d], Mei Zhen[c], Thomas Boulin[e] and Shangbang Gao[a,d,*]

[a]Key Laboratory of Molecular Biophysics of the Ministry of Education, College of Life Science and Technology, Huazhong University of Science and Technology, Wuhan 430074, China
[b]College of Biomedical Engineering, South-Central University for Nationalities, Wuhan 430074, China
[c]Lunenfeld-Tanenbaum Research Institute, Mount Sinai Hospital, University of Toronto, Toronto, ON M5G 1X5, Canada
[d]Department of Geriatrics, Tongji Hospital of Tongji Medical College, Huazhong University of Science and Technology, Wuhan 430030, China
[e]Univ Lyon, Université Claude Bernard Lyon 1, MeLiS, CNRS UMR 5284, INSERM U1314, Institut NeuroMyoGène, Lyon 69008, France
[f]King Abdullah University of Science and Technology (KAUST), Biological and Environmental Sciences and Engineering Division (BESE), Thuwal 23955–6900, Kingdom of Saudi Arabia
*To whom correspondence should be addressed: Email: sgao@hust.edu.cn
[1]Z.Y., Y.L., B.Y., and Y.X. contributed equally to this work.
Edited By: Gerhard Hummer

Abstract

Leak potassium (K^+) currents, conducted by two-pore domain K^+ (K_{2P}) channels, are critical for the stabilization of the membrane potential. The effect of K_{2P} channels on motor rhythm remains enigmatic. We show here that the K_{2P} TWK-40 contributes to the rhythmic defecation motor program (DMP) in *Caenorhabditis elegans*. Disrupting TWK-40 suppresses the expulsion defects of *nlp-40* and *aex-2* mutants. By contrast, a gain-of-function (*gf*) mutant of *twk-40* significantly reduces the expulsion frequency per DMP cycle. In situ whole-cell patch clamping demonstrates that TWK-40 forms an outward current that hyperpolarize the resting membrane potential of dorsorectal ganglion ventral process B (DVB), an excitatory GABAergic motor neuron that activates expulsion muscle contraction. In addition, TWK-40 substantially contributes to the rhythmic activity of DVB. Specifically, DVB Ca^{2+} oscillations exhibit obvious defects in loss-of-function (*lf*) mutant of *twk-40*. Expression of TWK-40(*gf*) in DVB recapitulates the expulsion deficiency of the *twk-40(gf)* mutant, and inhibits DVB Ca^{2+} oscillations in both wild-type and *twk-40(lf)* animals. Moreover, DVB innervated enteric muscles also exhibit rhythmic Ca^{2+} defects in *twk-40* mutants. In summary, these findings establish TWK-40 as a crucial neuronal stabilizer of DMP, linking leak K_{2P} channels with rhythmic motor activity.

Keywords: *twk-40*, K_{2P} channel, motor rhythm, Ca^{2+} oscillation, membrane potential

Significance Statement

Rhythmic motor programs, with durations ranging from milliseconds to hours, are critical for numerous physiological processes. However, the molecular mechanisms that maintain these rhythms remain elusive. This study uncovers the role of an endogenous leak K^+ channel, encoded by the gene of *twk-40*, in sustaining the defecation rhythm. We demonstrate that TWK-40 influences both the Ca^{2+} oscillations and the membrane potential within the dorsorectal ganglion ventral process B (DVB) neuron. Thus, TWK-40 is a vital component that affects the DVB neuron's transmission of pacemaker signals from the intestine to the enteric muscles. Given the K_{2P} channels' conserved function in modulating neuronal activity, our findings suggest their wider importance in regulating various rhythmic behaviors, such as respiration, cardiac pulsation, and gastrointestinal motility, in mammals.

Introduction

Two-pore domain potassium (K_{2P}) channels conduct K^+ leak currents. In contrast to voltage-gated K^+ channels, K_{2P} channels are mostly voltage-independent and noninactivating channels, which stabilize the cell's resting membrane potential (RMP) (1). Along with most K_{2P} channels profiling by heterologous expression systems or in cultured primary cells, the channel associated behaviors and the intrinsic physiological characterization of specific K_{2P} channel have remained largely unknown.

The human genome encodes 15 K_{2P} channels, which are grouped into six families based on their functional resemblance and structural similarity (2, 3). Aberrant functions of K_{2P} channels have been implicated in various disorders associated with genetic variation. For example, mutations of human TASK-3 (KCNK9

Competing Interest: The authors declare no competing interest.
Received: February 19, 2024. **Accepted:** June 5, 2024

p.Gly236Arg) cause *KCNK9* Imprinting Syndrome, a pediatric neurodevelopmental disease with severe feeding difficulties, delayed development and intellectual disability (4). With predicted conservation of amino acid sequences across species, K_{2P} channels associated genetic and functional investigations in animal models are emerging (5, 6). For instance, cardiac-specific inactivation or overexpression of Ork1, a *Drosophila* two-pore domain potassium channel, led to an increase or a complete arrest of fly heart beating, respectively (6).

The nematode *Caenorhabditis elegans* (or *C. elegans*) genome contains a large family with at least 47 K_{2P} genes (5, 7). This large set of K_{2P} channels may allow for exceptionally fine "tuning" of the firing activity of individual cells within the very compact nematode nervous system (8, 9). Encouraged by the increasing understanding of the molecular and cellular wiring of the worm's neural network (7, 9, 10, 11), we use *C. elegans* to explore the functional complexity of K_{2P} channels as potential regulators of rhythmic motor behaviors in vivo (12, 13).

The *C. elegans* defecation motor program (DMP) exhibits a highly coordinated ultradian rhythm. It is achieved by periodically activating a stereotyped sequence of muscle contractions, including the initial contraction of posterior body wall muscles (pBoc), followed by the second contraction of anterior body wall muscles (aBoc), and the final contraction of enteric muscles (EMC) (14). Driven by the synchronizing activity of electrically coupled dorsorectal ganglion ventral process B (DVB) and anterior ventral process L (AVL) motor neurons (15), EMC leads to the robust expulsion (Exp) of gut contents (Fig. 1A) (16, 17). Unlike most rhythmic motor circuits that are composed of a central pattern generator neural network or self-oscillating pacemaker neurons (18), the expulsion rhythm is precisely timed by endogenous calcium oscillation signals from the intestine (19, 20). The intestinal IP_3 receptor/*itr-1*-driven pacemaker Ca^{2+} oscillations trigger a Ca^{2+}-dependent secretion of neuropeptide NLP-40, which activates the neuronal G-protein-coupled receptor (GPCR) AEX-2 in DVB and AVL (21–24). GABA release from DVB (25), cyclically initiated by NLP-40 (24), activates the muscular excitatory GABA-gated cation channel EXP-1 to drive the final EMC (Fig. 1B) (26). Deficiency of either NLP-40, AEX-2 or EXP-1 results in serious expulsion defects in *C. elegans*. Although the intestinal Ca^{2+} oscillation sets the instructive timing signal of the expulsion rhythm (19, 20), the cellular processes that control the expulsion rhythm in the intestine-neuron-muscle circuit are still unclear.

We show here that loss of function of *twk-40*—a two-pore domain potassium channel subunit—specifically suppresses the expulsion defects of *nlp-40* and *aex-2* mutants, but not of *exp-1* mutant. TWK-40 exhibits the common structural features of K_{2P} channel based on sequence analyses (27–29). The single subunit of TWK-40 has four transmembrane regions and two pore-forming domains (Fig. 1I), which exhibit sequence similarity with the mammalian TASK (tandem-pore-acid-sensing K^+) subfamily (Fig. S1A). A gain of function mutant of *twk-40(bln336, L159N)*, similar to hTWIK(L146N) and hTASK1/3(L122N) that generated by CRISPR/Cas9 gene editing (12), induces an expulsion defect by reducing the frequency of expulsion per DMP cycle. Moreover, in situ whole-cell patch clamping revealed a *twk-40*-dependent outward K^+ current that regulates the RMP in DVB neurons, in which the RMP was depolarized in *twk-40(lf)* and hyperpolarized in *twk-40(L159N, gf)* mutant, respectively. In combination with real-time Ca^{2+} imaging, we provide several lines of evidence to demonstrate that TWK-40 contributes to rhythmic motor behaviors—including defecation—by cell-autonomously regulating DVB's activity.

Remarkably, our recent findings reveal that the TWK-40 K_{2P} channel plays a pivotal role in modulating global locomotor activity by influencing the activity of the AVA premotor interneuron (30). Specifically, animals with a loss-of-function (*lf*) mutation in *twk-40* exhibit exaggerated body bends during both forward and backward movement, and more frequent and prolonged reversals. In contrast, gain-of-function mutants of *twk-40* strongly altered locomotion including obvious decreased body bending and velocity in both forward and backward undulation. Therefore, the K_{2P} channel TWK-40 is required for multiple motor rhythms, including the defecation and locomotion motor programs.

Results

twk-40(lf) suppresses the expulsion defect of *nlp-40* and *aex-2* mutants

To determine a potential role of the TWK-40 K_{2P} channel in the cellular mechanisms controlling rhythmic DMP activity, we took advantage of three *exp* mutants that disrupt DMP in different tissues within the expulsion motor circuit (Fig. 1B). First, *nlp-40(tm4085)*, an instructive neuropeptide from the intestinal pacemaker that delivers temporal information to the DVB neuron (24). Second, *aex-2(sa3)*, a GPCR that functions as the DVB receptor for NLP-40 (21, 24). And the third, *exp-1(sa6)*, which encodes an excitatory GABA receptor expressed in enteric muscle (EM) (26, 31). *lf* mutants of these genes induced severe expulsion defects (Fig. 1C, E, G) by disrupting the normal function of the intestine, DVB neuron, and EM, respectively.

We reasoned that a loss of the potassium conductance *twk-40* would increase the excitability of cells within the circuit and compensate the inhibitory effect of the *nlp-40*, *aex-2*, or *exp-1* mutations. Hence, we combined the *twk-40* null allele *hp834* (30) with each DMP mutation. *hp834* contains a 7 bp deletion of the sequence (GTTCGAG) at the base of 127–133 exon before the first pore-forming domain of T28A8.1a (Fig. 1I), causing a frameshift and subsequent premature stop codon of *twk-40a* (30), one of three annotated isoforms of *twk-40* (www.wormbase.org). We term this mutant as *twk-40(hp834, lf)* or *twk-40(V65 deletion, LF)* (Fig. S1A). We found that *twk-40(V65, lf)* mutant significantly improved the expulsion defect in *nlp-40* and *aex-2* mutants (Fig. 1C–F). Specifically, the expulsion frequency per DMP was increased in *nlp-40(tm4085); twk-40(hp834)* (0.18 ± 0.02 Exp per cycle) or *aex-2(sa3); twk-40(hp834)* (0.15 ± 0.02 Exp per cycle), when compared to the single mutants of *nlp-40(tm4085)* (0.08 ± 0.01 Exp per cycle) and *aex-2(sa3)* (0.08 ± 0.01 Exp per cycle), respectively (Fig. 1C–F). Similar expulsion defect suppression was observed in another *twk-40(lf)* allele *hp733(E58K, LF)* (Fig. S1A, B), which harbors a missense mutation that changes an amino acid at the end of the first transmembrane domain (E58K) (30). By contrast, no substantial suppression of the expulsion defect of *exp-1* mutants was observed for either *lf* allele of *twk-40*. Indeed, no difference in expulsion frequency was observed between *exp-1(sa6)* (0.17 ± 0.01 Exp per cycle) and *exp-1(sa6); twk-40(hp834)* (0.17 ± 0.01 Exp per cycle) or *exp-1(sa6); twk-40(E58K, LF)* (0.16 ± 0.01 Exp per cycle) double mutants, respectively (Figs. 1G, H and S1B). These results demonstrated that *twk-40* is selectively required for rhythmic defecation regulation, upstream of *exp-1*.

A *twk-40* gain-of-function mutation reduces expulsion frequency

The selective suppression of *exp* defects in distinct *exp* mutants suggested that *twk-40*, per se, may contribute to the DMP.

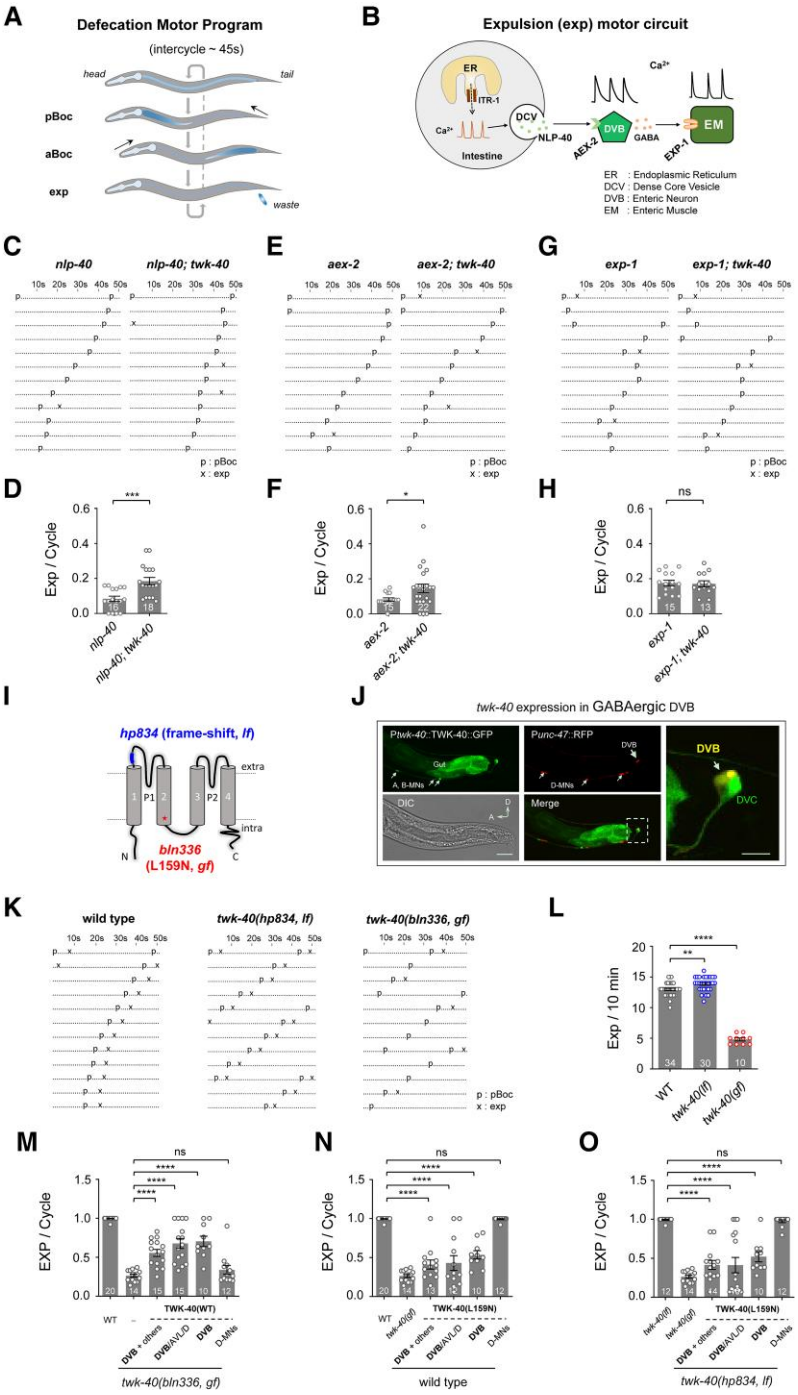

Fig. 1. Disrupted expulsion rhythm in *twk-40* mutants. A) Schematic representation of the defecation motor program (DMP), which consists of three distinct sets of muscle contractions: the posterior body muscle contraction (pBoc), the anterior body muscle contraction (aBoc), and the expulsion muscle contraction (exp or EMC). The regular defecation cycle period is approximately 45 s. B) Schematic representation of the expulsion motor circuit, including the intestine, DVB neuron, and EM. ER, endoplasmic reticulum; ITR-1, inositol 1,4,5-trisphosphate receptor; DCV, dense core vesicle. C, E, G) Ethograms of defecation behavior in *nlp-40* and *nlp-40; twk-40* double mutants, *aex-2* and *aex-2; twk-40* double mutants, and *exp-1* and *exp-1; twk-40* double mutants, respectively. Each dot and character represent 1 s. Letters "p" and "x" represent pBoc and exp, respectively. D, F, H) Quantifications of the expulsion frequency per defecation cycle. The expulsion deficiency was partially recovered by loss of *twk-40* in *nlp-40* and *aex-2* mutants, but not in *exp-1* mutants. I) Diagram of the TWK-40 K^+ channel and the mutation loci. P1 and P2, pore domains; 1–4 transmembrane domains; *fs*, predicted frameshift mutation; *gf*, gain-of-function mutation. J) *twk-40* is expressed in DVB based on co-localization of P*twk-40*::TWK-40::sl2dGFP and P*unc-47*::RFP. GFP was observed in the ventral excitatory motor neurons, a few head and tail neurons, and the intestine. Scale bar, 20 μm. *Right*, zoomed view of *twk-40* expression in DVB and DVC. Scale bar, 5 μm. K) Ethograms of defecation behavior in wild type, *twk-40(bln336, gf)* and *twk-40(hp834, lf)* animals. Each dot and character represent 1 s. Letters "p" and "x" represent pBoc and exp, respectively. L) Quantifications of the expulsion frequency per defecation cycle. Compared to wild-type animals, the expulsion deficiency was significantly reduced in *twk-40(bln336, gf)*, but not in *twk-40(hp834, lf)*. M) Neuronal expression of wild-type TWK-40 (TWK-40(WT)) in DVB neurons rescues the expulsion deficiency of *twk-40(bln336, gf)* mutants. N, O) Neuronal expression of gain-of-function TWK-40(L159N) in DVB in wild type (N) or *twk-40(hp834, lf)* (O) recapitulates the expulsion deficiency of *twk-40(gf)* mutant. The number of tested animals is indicated for each strain. All data are expressed as means ± SEM. One-way ANOVA test was used, in which: ns, not significant, $^{**}P < 0.01$, $^{*}P < 0.05$, $^{***}P < 0.001$, $^{****}P < 0.0001$ relative to wild type or as indicated.

Indeed, in *twk-40(V65 deletion)* single mutants, the expulsion number was modestly but significantly increased (13.87 ± 0.21/10 min) compared to wild-type animals (12.97 ± 0.19/10 min) (Fig. 1K, L). Similar results were also observed in *twk-40(E58K, LF)* mutants. These results confirm that *twk-40* contributes to the DMP negatively.

To further confirm the involvement of *twk-40* in the DMP, we examined the expulsion step in a gain-of-function mutant allele of *twk-40, bln336(L159N, GF)* (Fig. 1I). These mutants harbor a pan-K_{2P} activating mutation (12) that promotes the gating of vertebrate and invertebrate K_{2P} channels. Indeed, heterologous expression of the corresponding TWK-40(L159N, GF) channel in HEK293T cells showed ~5 fold current increase from the wild-type TWK-40 (30). Consistent with an inhibitory function of *twk-40*, we observed a strongly reduced expulsion frequency (4.8 ± 0.25/10 min) in *twk-40(bln336, L159N)* animals, i.e. approximately 25% of wild type (12.97 ± 0.19/10 min) (Fig. 1K, L). Thus, gain-of-function of *twk-40* inhibits the expulsion rhythm, which encouraged us to further investigate the functional effects of *twk-40* loss- and gain-of-function mutants.

twk-40 mutants disrupt the expulsion behavior

To pinpoint the exact role of *twk-40* in the DMP, we first assessed its cellular focus of action. Loss of *twk-40* suppressed the *exp* defect of *nlp-40* and *aex-2* mutants but not of *exp-1*, indicating that *twk-40* mutants disrupt the expulsion frequency from the intestine and/or expulsion neurons. Indeed, functional TWK-40 driven by a small fragment of its upstream region (P*twk-40*::TWK-40::sl2dGF) (Tables S1–S3) revealed the expression exclusively in the nervous system and intestine (Fig. 1J). The neuronal expression pattern includes the excitatory ventral motor neurons (A- and B-types), and the excitatory GABAergic DVB motor neuron/interneuron (moderate), but no expression was observed in inhibitory D-motor neurons. Meanwhile, sparse labeling of head and tail neurons was also observed, including the DVC interneuron (strong) (Fig. 1J).

We then systematically tested the tissue or cell requirements of *twk-40* for the expulsion behavior. A wild-type TWK-40 cDNA driven by different promoters was competitively expressed in *twk-40(L159N, gf)* mutant (0.26 ± 0.02 Exp per cycle), in an attempt to reduce its severe *exp* defect. Expression of wild-type TWK-40 (i.e. TWK-40(WT)) by the short promoter P*twk-40* (Tables S2 and S3) rescued the animal's expulsion frequency to (0.55 ± 0.04 Exp per cycle) (Fig. 1M). Expression of TWK-40(WT) in GABAergic DVB/AVL/D-motor neurons (P*unc-47*), also significantly restored the DMP (0.67 ± 0.06 Exp per cycle). More importantly, when we restored TWK-40(WT) expression exclusively in the DVB neuron (P*flp-10*) (15), the expulsion defect of *twk-40(L159N, gf)* mutant was rescued (0.7 ± 0.06 Exp per cycle). In contrast, expression of the TWK-40(WT) in the intestine (P*ges-1*, 33.2 ± 1.9%) (Fig. S1C) or D-motor neurons (P*unc-25* s, 33.8 ± 5.6%) (32), however, did not restore a normal expulsion frequency (Fig. 1M). Therefore, consistent with the expression pattern, these results suggest that regulation of the expulsion rhythm by *twk-40* requires DVB neurons.

To further confirm this notion, we ectopically expressed the TWK-40(L159N) gain-of-function mutant in DVB neurons. Indeed, in the wild-type N2 background, TWK-40(L159N) expression in DVB (P*twk-40*, P*unc-47* or P*flp-10*) resembled the expulsion defect as found in *twk-40(bln336, L159N)* mutant animals, exhibiting strongly reduced expulsion frequency per cycle (Fig. 1N). TWK-40(L159N) expression only in D-MNs (P*unc-25s*), however, could not replicate this defect. Similar phenotypes were also observed by expressing TWK-40(L159N) in a *twk-40(lf)* mutant context (Fig. 1O).

Taken together, these results demonstrate that *twk-40* is sufficient and necessary in DVB neurons for the regulation of the expulsion.

Aberrant Ca^{2+} oscillation of the DVB neuron in *twk-40* mutants

To determine whether *twk-40* directly mediates DVB's neuronal activity, we performed Ca^{2+} imaging in animals expressing the genetically encoded Ca^{2+} sensor GCaMP6s in the DVB neuron (Fig. 2A, Table S1) (33). We conducted the Ca^{2+} imaging in a liquid environment on restricted animals, in which DVB exhibited tight correlation of rhythmic Ca^{2+} oscillations with cyclic expulsion behavior (Fig. 2B–D). In wild-type animals, DVB fired periodic Ca^{2+} spikes (or Ca^{2+} oscillations) with a frequency of 4.5 ± 0.3 Hz/300 s (Fig. 2B, E, F). To verify these Ca^{2+} spikes represent pacemaker-activated DVB activation, we examined their dependence on NLP-40, the instructive neuropeptide from the intestinal pacemaker that delivers temporal information to the DVB neuron (24). Consistent with previous reports (15, 24), we observed severe decrease in both DVB Ca^{2+} and expulsion frequency in the *nlp-40(tm4085)* mutant (Fig. S2A–C). These results demonstrate that the activation dynamics of DVB are indeed dependent on the NLP-40-initiated pacemaker signal.

In *twk-40(L159N, gf)* mutants, the frequency of Ca^{2+} spikes was significantly reduced to 3.2 ± 0.3 Hz/300 s (Fig. 2E, F). Interestingly, the Ca^{2+} amplitude was also diminished in *twk-40(L159N, gf)* mutants (Fig. 2G). Conversely, in *twk-40(hp834, lf)* mutants, the Ca^{2+} frequency was significantly increased to 5.9 ± 0.5 Hz/300 s. Yet, the Ca^{2+} amplitude of *twk-40(hp834)* was unchanged (Fig. 2G), and the individual Ca^{2+} spike kinetics—including the rise and decay time—were not modified either (Fig. S3A–C), suggesting that *twk-40* contributes to the basal-activity of the DVB neuron. Taken together, our experiments demonstrate that the intrinsic DVB Ca^{2+} oscillation activity was substantially regulated by *twk-40*.

To further decipher *twk-40*'s cellular specificity, we firstly measured neuronal Ca^{2+} activity by expressing wild-type TWK-40 cDNA under different exogenous promoters in a *twk-40(L159N, gf)* mutant background (Tables S1–S3). Consistent with our behavioral data, the Ca^{2+} frequency and amplitude were partially rescued when TWK-40(WT) was expressed in DVB in *twk-40(L159N, gf)* mutants (Fig. 2H–J). By contrast, neither frequency nor amplitude was restored when TWK-40(WT) was expressed in D-motor neurons. In addition, we then expressed TWK-40(WT) in *twk-40(hp834, lf)* mutant and found that the increased Ca^{2+} frequency of these mutants could also be rescued to wild-type levels when TWK-40(WT) was expressed in DVB (Fig. 2K–M). Thus, TWK-40(WT) is sufficient to restore the neuronal Ca^{2+} activity of the DVB neurons.

Collectively, these results support the notion that *twk-40* mediates neuronal Ca^{2+} oscillations of the DVB neuron.

twk-40 cell-autonomously regulates DVB Ca^{2+} oscillation

The broad neuronal expression pattern of *twk-40* indicates that TWK-40 may contribute to the DMP not limited in the DVB neuron (11). To examine whether synaptic input upstream of DVB may play a role, we examined the DVB Ca^{2+} oscillations in an *unc-13(lf)* background (24). UNC-13 is a conserved and essential presynaptic

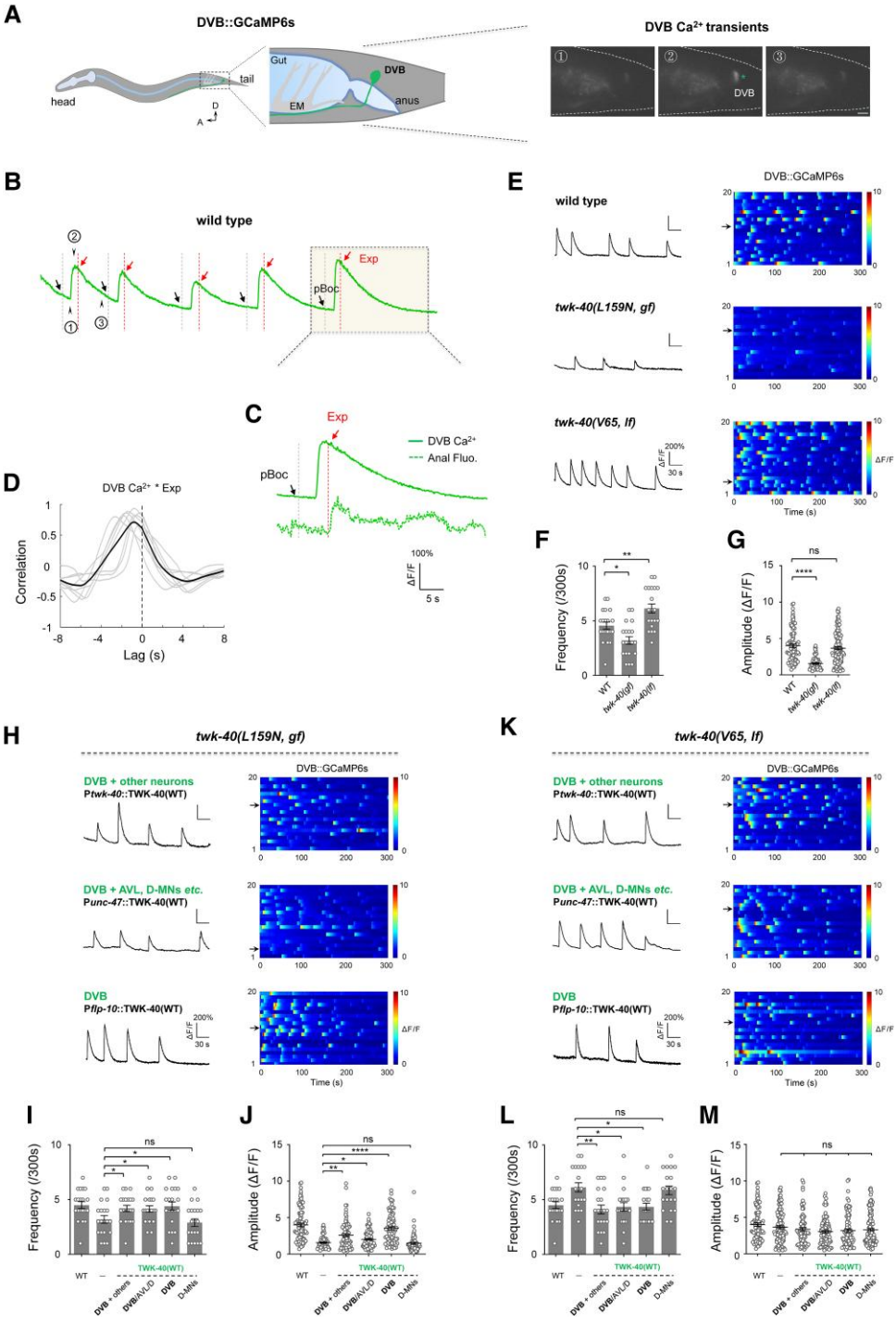

Fig. 2. TWK-40 inhibits DVB Ca^{2+} oscillation. A) *Left*, schematic representation of *C. elegans* DVB neuron and enteric muscle (EM) in a lateral view. The genetically encoded Ca^{2+} indicator GCaMP6s was expressed in DVB to measure its neuronal activity. *Right*, representative spontaneous Ca^{2+} oscillation imaged by GCaMP in DVB neuron. From left to right, Ca^{2+} signal of DVB in (1) the quiescent state, (2) at peak Ca^{2+} signal, and (3) upon return to the basal state. Scale bar, 5 μm. B) Representative recording of Ca^{2+} oscillations in DVB over time. Arrow heads indicate the corresponding time points in upper panels. C) Representative single event of simultaneous recording of DVB Ca^{2+} activity and expulsion action that observed by anal bacterial fluorescence. D) Cross-correlation between DVB Ca^{2+} and Exp. Faint lines indicate the results from individual Ca^{2+} transient, and the black line indicates mean value. Black dashed line denotes tight correlation between DVB Ca^{2+} and Exp action with a ~0.8 s delay. E) Representative Ca^{2+} activity (*left*) and color maps (*right*) of DVB neurons in wild type, *twk-40(bln336, gf)* and *twk-40(hp834, lf)* mutants, respectively. F, G) Significant reduction of Ca^{2+} transient frequency and amplitude in *twk-40(bln336, gf)* mutant, $n = 20$. Reduction of frequency but not amplitude in *twk-40(hp834, lf)* mutants. H) Representative DVB Ca^{2+} traces (*left*) and color maps (*right*) for tissue-specific expression of TWK-40(WT) in *twk-40(bln336, gf)* mutants: endogenous promoter P*twk-40*, P*unc-47* promoter including DVB/AVL/D-MNs expression, P*flp-10* promoter for DVB specific expression, P*unc-25s* promoter including D-MNs/RME expression but lacking DVB expression. I, J) Quantification of the frequency and amplitude of Ca^{2+} transients, $n = 20$. K) Representative DVB Ca^{2+} traces (*left*) and color maps (*right*) for tissue-specific expression of TWK-40(WT) in *twk-40(hp834, lf)* mutant. L, M) Quantification of the frequency and amplitude of Ca^{2+} transients, $n = 20$ animals. All data are expressed as means ± SEM. One-way ANOVA test was used, in which: ns, not significant, $^{*}P < 0.05$, $^{**}P < 0.01$, $^{****}P < 0.0001$ in comparison with that as denoted.

Ca^{2+} effector that triggers exocytosis and neurotransmitter release (34–36). Loss of function of *unc-13* strongly impairs global neurotransmission with minor effect on NLP-40 release (24). Interestingly, in the *unc-13(lf)* mutant background, we found that Ca^{2+} oscillation defects were retained in *twk-40* mutants, including the decreased frequency and amplitude in *twk-40(L159N, gf)* mutants and increased frequency in *twk-40(hp834, lf)* mutants (Fig. S4A–C). These results demonstrate that potential presynaptic inputs to DVB do not interfere with the regulation of DVB's Ca^{2+} activities by TWK-40, and that *twk-40* most likely regulates the cellular excitability of DVB neuron in a cell-autonomous manner.

To reinforce this notion, we further tested TWK-40's inhibition of DVB by measuring the Ca^{2+} oscillation in different transgenic lines that expressed the *twk-40(L159N, gf)* cDNA. When TWK-40(L159N) was expressed in DVB in wild-type animals (P*twk-40*, P*unc-47* or P*flp-10*), the frequency and amplitude of Ca^{2+} spikes were significantly reduced (Fig. S5A), similar to *twk-40(L159N, gf)* mutants (Fig. S5B, C). By contrast, expression of TWK-40(L159N) in D-motor neurons had no effect. Furthermore, reduced Ca^{2+} oscillations were also observed when TWK-40(L159N) was expressed in a *twk-40(hp834, lf)* mutant background (Fig. S5E, F). These results reveal that ectopic expression of TWK-40(L159N) is sufficient to silence the Ca^{2+} oscillation of DVB neurons. Namely, TWK-40 execute a dominant inhibition of the intrinsic activity regulation in DVB neuron.

DVB activity regulates Ca^{2+} dynamics in enteric muscles

The expulsion behavior ultimately relies on the coordinated contraction of a group of muscles, including the anal depressor and sphincter, and two EM, which wrap around the posterior gut to further pressurize the intestinal contents (25). EMs are innervated by DVB (Fig. 3A) and AVL neurons (11, 25), and the contraction of EMs is driven by intracellular Ca^{2+} transients (37). We then ask whether EM Ca^{2+} activity is also disrupted in *twk-40* mutants.

We thus performed Ca^{2+} imaging of animals expressing the calcium indicator GCaMP6s in the enteric muscles (EM::GCaMP6s, Fig. 3B) (33). Similar to activation dynamics in DVB neuron, EM displayed rhythmic Ca^{2+} spikes closely correlated with expulsion action (Fig. 3C, D). In our experimental conditions, the EM Ca^{2+} spikes exhibited a frequency of 6.4 ± 0.5 Hz/300 s ($n = 20$) in wild-type animals (Fig. 3E), which was also eliminated in *nlp-40(tm4085)* mutant (Fig. S2D, E). In *twk-40* mutants, the periodicity of EM Ca^{2+} spikes was affected. Specifically, the EM Ca^{2+} frequency was significantly reduced in *twk-40(L159N, gf)* mutants (3.0 ± 0.2 Hz/300 s, $n = 20$), and increased to 8.6 ± 0.6 Hz/300 s ($n = 20$) in *twk-40(hp834, lf)* mutants (Fig. 3E, F), reminiscent of *twk-40*'s effects for DVB Ca^{2+} frequency. EM Ca^{2+} amplitudes, however, were unchanged in *twk-40(L159N, gf)* animals (Fig. 3G), which differs from the reduction observed for DVB Ca^{2+} spike amplitudes. Given that no *twk-40* expression was observed in EM, we propose that the effects of *twk-40* mutations on the Ca^{2+} activity of EM are a consequence of the dysregulation of presynaptic DVB neurons.

To confirm this idea, we performed additional experiments by expressing wild-type TWK-40 in EM and DVB neurons, respectively. We found that the reduced EM Ca^{2+} frequency in *twk-40(L159N, gf)* mutant was almost fully rescued by expressing TWK-40(WT) in DVB (P*twk-40*, P*unc-47* and P*flp-10*), but not in EM (P*exp-1*) or in D-motor neurons (P*unc-25s*) (Fig. 3H, I). Consistently, the increased frequency of EM Ca^{2+} spikes in *twk-40(hp834, lf)* mutants was also restored to wild-type by TWK-40(WT) expression in DVB neurons (Fig. 3J, K). We also ectopically expressed the gain-of-function TWK-40(L159N) in *twk-40(hp834)* animals to inhibit DVB's activity and recorded the EM Ca^{2+} spikes. Consistently, the frequency of EM Ca^{2+} spikes was significantly diminished in this experiment. This inhibition was however not observed in animals expressing TWK-40(L159N) in the EM or D-motor neurons (Fig. 3L, M). Collectively, our experiments argue that *twk-40* changes Ca^{2+} activities of EM by modulating DVB activity.

TWK-40 hyperpolarizes the RMP of DVB neuron

The functional inhibition of DVB neuron by *twk-40* is consistent with an inhibitory function of this potassium channel. To directly investigate the functional effect of *twk-40*, we dissected and recorded GFP-labeled DVB neurons in vivo in the whole-cell patch clamp configuration (Fig. 4A). In wild-type animals, stable outward K^+ currents were recorded at stepwise holding voltages from −60 mV to +80 mV (38, 39). These currents were significantly diminished in *twk-40(hp834) lf* mutants (Fig. 4B, C). Conversely, in *twk-40(L159N)* gain-of-function mutants, outward currents were dramatically increased (Fig. 4B, C). Thus, these in situ neuronal recordings demonstrate that *twk-40* supports a functional K^+ current in DVB neuron.

Furthermore, the RMP of DVB was also analyzed. While wild-type DVB neurons had an RMP of -38.9 ± 3.7 mV ($n = 6$), loss of *twk-40* depolarized the RMP to -22.1 ± 2.9 mV ($n = 7$). Conversely, in *twk-40(L159N, gf)* mutants, the RMP of DVB neuron was dramatically hyperpolarized to -63.1 ± 5.8 mV ($n = 6$) (Fig. 4D, E). Taken together, these results demonstrate that TWK-40 constitutes a K^+ channel that stabilizes the RMP of DVB neuron.

In summary, we show here that TWK-40 forms a *bona fide* potassium channel that cell-autonomously maintains the RMP of DVB neuron, and that *twk-40* is essential for the regulation of the rhythmic expulsion motor program (Fig. 4F).

Discussion

Potassium currents mediated by K_{2P} channels are important modulators of neuronal activity in animal nervous systems. We show here that the previously uncharacterized K_{2P} channel TWK-40 provides a prominent leak potassium current in the DVB motor neuron that regulates the rhythmic expulsion behavior of *C. elegans*. We present genetic evidence that loss of *twk-40* suppresses the *exp* defects of *nlp-40* and *aex-2* mutants. Additional evidence from behavioral rescue experiments, and real-time neuronal and muscular Ca^{2+} imaging, reveal the substantial contribution of TWK-40 to rhythmic expulsion activity. Further proof collected by in situ whole-cell patch clamp recording and heterologous expression of TWK-40 (30), demonstrates that *twk-40* constitutes a neuronal K_{2P}-like potassium-selective current. Our results thus identify a K_{2P} channel TWK-40, through its influence on DVB neuron (this study) and AVA interneuron (30), plays a critical role in coordinating the expulsion rhythm and locomotion, respectively. These findings suggest a broader significance of TWK-40/K_{2P} in orchestrating multiple motor rhythms, providing insights into the molecular mechanisms underlying coordinated motor behaviors.

Genetic analysis initially highlighted critical ion channel genes for DVB activity, such as *unc-2* and *egl-19* that encode the α1 subunits of P/Q- and L- type voltage-gated Ca^{2+} channel, respectively (40), and *egl-36*, a Shaw-type (Kv3) voltage-dependent potassium channel subunit (41). However, the in vivo cellular mechanism of how these channels contribute to the behavior is unknown. The recent descriptions of synchronized giant action potentials

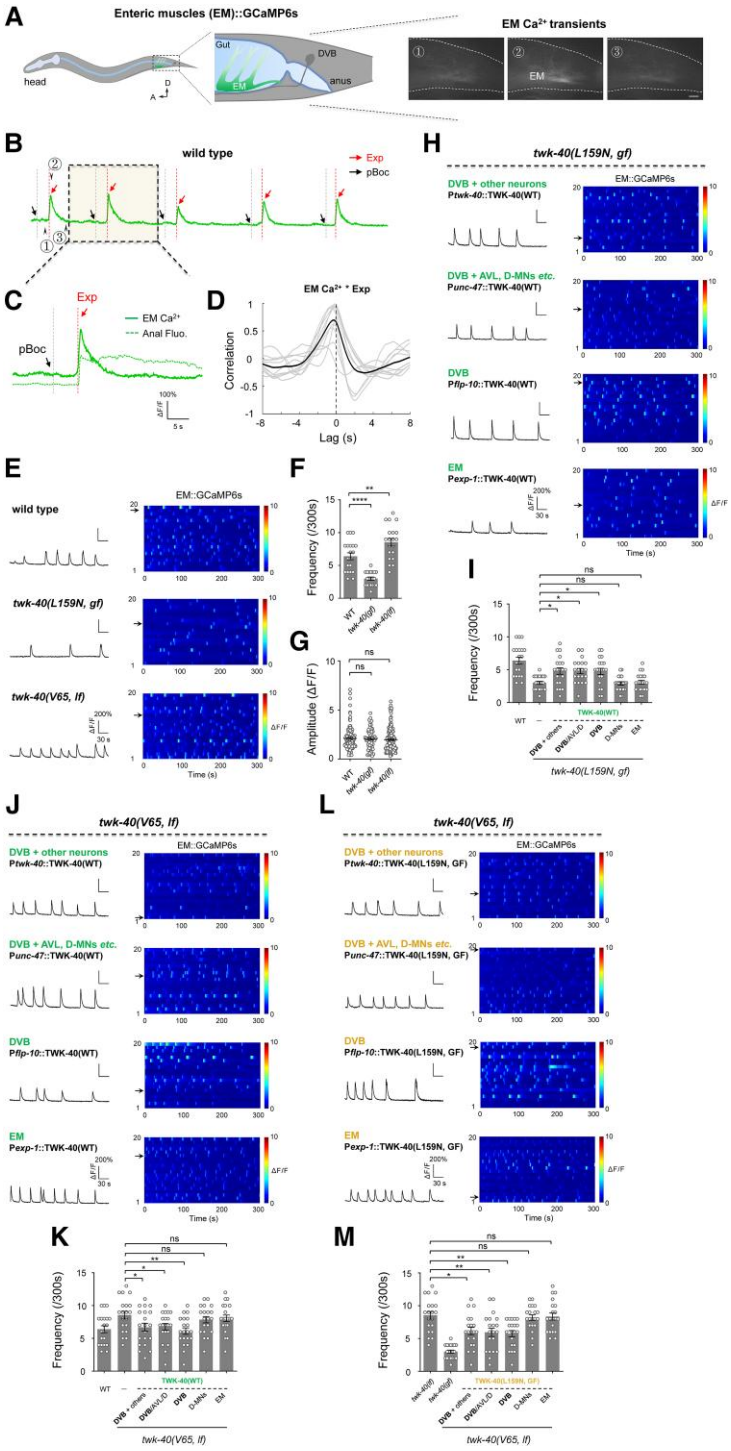

Fig. 3. DVB-driven Ca^{2+} dynamics in enteric muscles was altered in *twk-40* mutants. A) *Left*, schematic representation of *C. elegans* DVB neuron and enteric muscle (EM) in a lateral view. *Right*, representative Ca^{2+} oscillation imaged by GCaMP in EM in vivo. From left to right, Ca^{2+} signal of EM in the quiescent state, at peak Ca^{2+} signal and upon return to the basal state. Scale bar, 5 μm. B) Representative recording of Ca^{2+} oscillations in EM over time. C) Representative single event of simultaneous recording of EM Ca^{2+} activity and expulsion action that observed by anal bacterial fluorescence. D) Cross-correlation between EM Ca^{2+} and Exp. Black dashed line denotes tight correlation between EM Ca^{2+} and Exp action with a ~0.3 s delay. E) Representative Ca^{2+} activity (*left*) and color maps (*right*) of enteric muscles in *twk-40(bln336, gf)* and *twk-40(hp834, lf)* mutants, respectively. F, G) Quantification of EM Ca^{2+} transients frequency and amplitude, $n = 20$. Ca^{2+} transient frequency was significantly reduced in *twk-40(bln336, gf)* mutant but was increased in *twk-40(hp834, lf)* mutant. EM Ca^{2+} amplitude was not altered in either mutants. H, J) Representative EM Ca^{2+} traces (*left*) and color maps (*right*) in *twk-40(bln336, gf)* and *twk-40(hp834, lf)* for tissue-specific expression of TWK-40(WT). Different promoters are used: 1, endogenous promoter P*twk-40*; 2, P*unc-47* promoter including DVB/AVL/D-MNs expression; 3, P*flp-10* promoter for DVB specific expression; 4, P*unc-25s* promoter including D-MNs/RME expression but lacking DVB expression; 5, P*exp-1* promoter for enteric muscle expression. I, K) Rescue of EM Ca^{2+} transient frequency by expression of TWK-40(WT) in DVB, but not enteric muscles or other neurons, $n = 20$. L) Representative EM Ca^{2+} traces (*left*) and color maps (*right*) in *twk-40(hp834, lf)* following tissue-specific expression of TWK-40(L159N). M) Reduction of EM Ca^{2+} transient frequency following TWK-40(L159N) expression in DVB, but not in enteric muscles or other neurons, $n = 20$. All data are expressed as means ± SEM. One-way ANOVA test was used, in which: ns, not significant, $^{*}P < 0.05$, $^{**}P < 0.01$, $^{****}P < 0.0001$ in comparison with that as denoted.

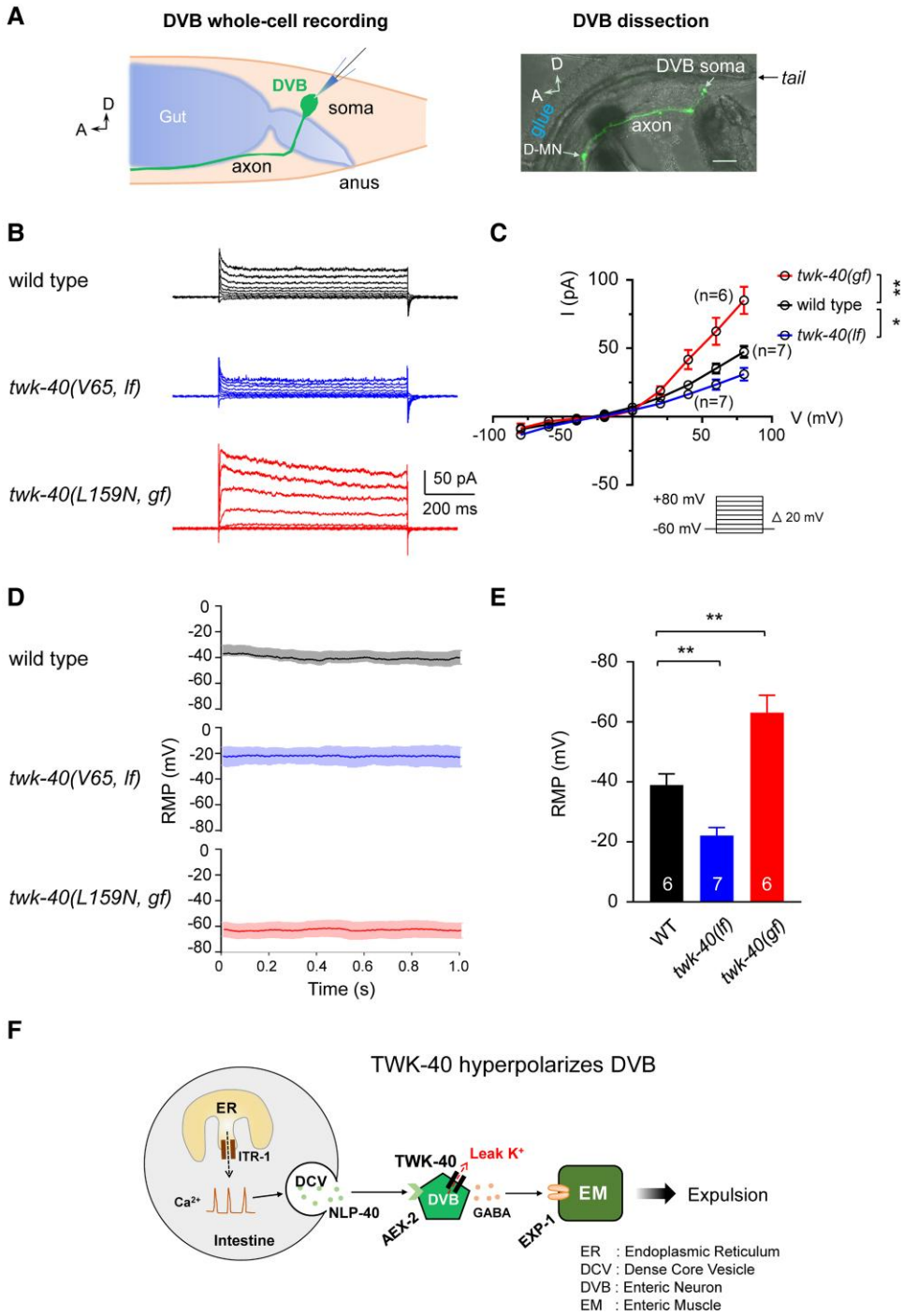

Fig. 4. TWK-40 hyperpolarizes the membrane potential of DVB neuron. A) *Left*, schematic representation of *C. elegans* DVB neuron for whole-cell patch clamp recording. *Right*, GFP-labeled DVB soma and axon. B) Representative outward K^+ currents recorded from DVB neurons in different genotypes. C) Quantification of the current–voltage curves from different genotypes reveals that the outward currents were reduced in *twk-40(hp834, lf)* mutant, but increased in *twk-40(bln336, gf)* mutant. D, E) Representative traces and quantification of the resting membrane potential (RMP) recorded from DVB in different genotypes. F) The working Model: K_{2P} channel TWK-40 participate in the regulation of rhythmic expulsion behavior by setting the RMP of DVB neuron. One-way ANOVA test was used to test the significant difference of average currents at +80 mV, in which: ns, not significant, $^*P < 0.05$, $^{**}P < 0.01$ in comparison with that as denoted.

between AVL and DVB, and of unusual compound action potentials in AVL, provide insights into how the rhythmic expulsion behavior is generated at the cellular level. In particular, the negative potassium spikes in AVL are mediated by a repolarization-activated potassium channel EXP-2 (38). This study identifies how the TWK-40 channel contributes to DVB's rhythmic activity, at the interface between the pace-making intestinal tissue and EM. Moreover, the interplay between AVL and DVB neurons, mediated through gap junction coupling, is crucial for the generation of action potentials in DVB (38). TWK-40 may possibly interact with components of the gap junction complex or be modulated by the coupling activity itself.

Among 47 K_{2P} genes in the *C. elegans* genome (7), only few have been substantially investigated. Interestingly, nematode K_{2P}

channels have been mostly studied using gain-of-function mutations identified in forward genetic screens. For instance, while *twk-18(gf)* mutants cause sluggish, uncoordinated movement (42), *sup-9(gf)* mutants are hyperactive with a characteristic rubberband phenotype (43). Gain-of-function mutants of *unc-58* show significant deficits in locomotion, egg laying, development, and aging (44, 45). Except for *twk-18*, we still lack a comprehensive understanding of the electrical properties of these channels in vitro and in vivo. The recent discovery of a universal activating mutation that promotes the gating of vertebrate and invertebrate K_{2P} channels has opened the way to more comprehensive manipulation of ion channel activity (12). We used this strategy here to engineer a point mutation of TWK-40 L159N that achieved a substantial gain-of-function effect. First, we show in a related study that the currents conducted by TWK-40(L159N) channels exhibit ~5-fold increase compared to TWK-40(WT) when heterologously expressed in HEK293 cells (30). Second, the RMP of DVB neurons was drastically hyperpolarized due to the increased outward K^+ current. In this *twk-40(L159N)* gain-of-function mutant, the neuronal Ca^{2+} oscillation frequency and amplitude were also reduced, resulting in the significantly diminished expulsion frequency. Thus, our study not only identifies TWK-40 as a regulator of the expulsion rhythm and DVB RMP but also provides biophysical insight into the electrical properties of the K_{2P} channel.

We also describe the impact of loss of *twk-40* on the expulsion behavior and DVB activity. In contrast to *gf* mutants, the RMP of DVB neuron was depolarized in *twk-40(lf)* mutant, and high Ca^{2+} oscillation activity was observed. Consequently, the expulsion number exhibited a moderate but significant increase in *twk-40(lf)* mutant. The fact that only few K_{2P} mutants with loss of function phenotypes have been identified in *C. elegans* may be due to functional redundancy between K_{2P} genes. *twk-7* is a notable exception as it exhibits hyperactive locomotion (46, 47). Interestingly, we have found that *twk-40(lf)* mutants also exhibit increased forward and backward body bends, as well as more frequent and prolonged reversals (30). A recent genetic study reported that loss of function *twk-40* could reverse the reduced body curvature of *C. elegans NALCN(lf)* mutants (48). Thus, TWK-40 is required for the regulation of multiple motor rhythms.

Although the expression of *twk-40* on DVB does not appear to be the highest from both our data and CeNGEN (https://www.cengen.org), direct whole-cell recording of DVB showed that *twk-40* significantly modulated the outward K^+ current. The slight outward-rectification of the *twk-40* dependent K^+ currents in DVB neurons differs from the voltage-independent currents observed in recombinant TWK-40 recorded in HEK293 cells (30). This could be due to endogenous regulatory subunits expressed in DVB neurons that modify the channel kinetics of TWK-40. Alternatively, TWK-40 could form heteromers with other K_{2P} subunits in vivo, resulting in heterodimers with different activation kinetics (49). A potential dynamic regulation of TWK-40, controlled by intracellular signaling pathways such as those mediated by cAMP in response to the activation of the GPCR AEX-2 (24, 40), or by extracellular molecular like protons released from intestine to initiate pBoc (50), could also modulate its activation kinetics and represent a mechanism by which the neuron adapts to physiological demands, fine-tuning the transmission of the pacemaker signal in a context-dependent manner. Our study, in its current state, shows the influence of TWK-40 in the function of DVB neuron and rhythmic motor programs, however, this does not preclude the involvement of other channels because DVB expresses multiple K_{2P} channels (51).

K_{2P} channels can be modulated by a variety of biophysical parameters, such as pH, temperature, and mechanic forces (1). Certain K_{2P} channels, including TASK-1/3, TREK-1, and TRESK, are activated by volatile general anesthetics at clinically relevant concentrations (52–54), indicating a major class of drug target from these K_{2P} channels. While our current data do not directly address these possibility, future studies could investigate whether TWK-40 activity is altered by the molecules that respond to metabolic or neurotransmitter cues. As a possible ortholog of human TASK-1/3, identification of the critical stimulator of TWK-40 in the future could promote the understanding of how the external environment and internal state affect motor rhythm via K_{2P} channel.

Acknowledgments

We thank Wesley Hung for reagents, Chenhong Li for valuable discussion. We thank *Caenorhabditis Genetics Center*, which is funded by the NIH Office of Research Infrastructure Programs (P40 OD010440), for strains.

Supplementary Material

Supplementary material is available at *PNAS Nexus* online.

Funding

This work was supported by the Major International (Regional) Joint Research Project (32020103007), the National Natural Science Foundation of China (32371189, 31871069), the National Key Research and Development Program of China (2022YFA1206001), the Overseas High-level Talents Introduction Program, the Canadian Institute of Health Research (FDN154274), the Natural Sciences and Engineering Research Council of Canada (RGPIN2017-06738), and the European Research Council (TB, ERC Starting Grant, Kelegans).

Author Contributions

S.G. conceived experiments and wrote the manuscript. Z.Y., Y.L., B.Y., and Y.X. performed experiments and analyzed data. L.C., J.C. J.M., Y.W., Y.T., S.E.M., and C.Z. contributed to the experiments. M.Z. and T.B. provided reagents, discussed the experiments, and edited the text.

Preprint

This manuscript was posted on a preprint: https://doi.org/10.1101/2022.04.09.487752.

Data Availability

Data supporting the findings of this study are included within the article and the Supplementary material. All data set are publicly available via Zenodo (https://zenodo.org/records/11440010).

References

1 Enyedi P, Czirjak G. 2010. Molecular background of leak K^+ currents: two-pore domain potassium channels. *Physiol Rev*. 90: 559–605.
2 Goldstein SA, *et al.* 2005. International Union of Pharmacology. LV. Nomenclature and molecular relationships of two-P potassium channels. *Pharmacol Rev*. 57:527–540.

3 Lesage F, Lazdunski M. 2000. Molecular and functional properties of two-pore-domain potassium channels. *Am J Physiol Renal Physiol*. 279:F793–F801.
4 Graham JM Jr, *et al.* 2016. KCNK9 imprinting syndrome-further delineation of a possible treatable disorder. *Am J Med Genet A*. 170:2632–2637.
5 Buckingham SD, Kidd JF, Law RJ, Franks CJ, Sattelle DB. 2005. Structure and function of two-pore-domain K^+ channels: contributions from genetic model organisms. *Trends Pharmacol Sci*. 26: 361–367.
6 Lalevee N, Monier B, Senatore S, Perrin L, Semeriva M. 2006. Control of cardiac rhythm by ORK1, a *Drosophila* two-pore domain potassium channel. *Curr Biol*. 16:1502–1508.
7 Bargmann CI. 1998. Neurobiology of the *Caenorhabditis elegans* genome. *Science*. 282:2028–2033.
8 Salkoff L, *et al.* 2001. Evolution tunes the excitability of individual neurons. *Neuroscience*. 103:853–859.
9 Witvliet D, *et al.* 2021. Connectomes across development reveal principles of brain maturation. *Nature*. 596:257–261.
10 Cook SJ, *et al.* 2019. Whole-animal connectomes of both *Caenorhabditis elegans* sexes. *Nature*. 571:63–71.
11 White JG, Southgate E, Thomson JN, Brenner S. 1986. The structure of the nervous system of the nematode *Caenorhabditis elegans*. *Philos Trans R Soc B Biol Sci*. 314:1–340.
12 Ben Soussia I, *et al.* 2019. Mutation of a single residue promotes gating of vertebrate and invertebrate two-pore domain potassium channels. *Nat Commun*. 10:787.
13 Wang ZW, Kunkel MT, Wei A, Butler A, Salkoff L. 1999. Genomic organization of nematode 4TM K^+ channels. *Ann N Y Acad Sci*. 868:286–303.
14 Thomas JH. 1990. Genetic analysis of defecation in *Caenorhabditis elegans*. *Genetics*. 124:855–872.
15 Choi U, Wang H, Hu M, Kim S, Sieburth D. 2021. Presynaptic coupling by electrical synapses coordinates a rhythmic behavior by synchronizing the activities of a neuron pair. *Proc Natl Acad Sci USA*. 118:e2022599118.
16 Dal Santo P, Logan MA, Chisholm AD, Jorgensen EM. 1999. The inositol trisphosphate receptor regulates a 50-second behavioral rhythm in *C. elegans*. *Cell*. 98:757–767.
17 Liu DW, Thomas JH. 1994. Regulation of a periodic motor program in *C. elegans*. *J Neurosci*. 14:1953–1962.
18 Marder E, Calabrese RL. 1996. Principles of rhythmic motor pattern generation. *Physiol Rev*. 76:687–717.
19 Branicky R, Hekimi S. 2006. What keeps *C. elegans* regular: the genetics of defecation. *Trends Genet*. 22:571–579.
20 McIntire SL, Jorgensen E, Horvitz HR. 1993a. Genes required for GABA function in *Caenorhabditis elegans*. *Nature*. 364:334–337.
21 Mahoney TR, *et al.* 2008. Intestinal signaling to GABAergic neurons regulates a rhythmic behavior in *Caenorhabditis elegans*. *Proc Natl Acad Sci USA*. 105:16350–16355.
22 Nehrke K, Denton J, Mowrey W. 2008. Intestinal Ca^{2+} wave dynamics in freely moving *C. elegans* coordinate execution of a rhythmic motor program. *Am J Physiol Cell Physiol*. 294:C333–C344.
23 Teramoto T, Iwasaki K. 2006. Intestinal calcium waves coordinate a behavioral motor program in *C. elegans*. *Cell Calcium*. 40: 319–327.
24 Wang H, *et al.* 2013. Neuropeptide secreted from a pacemaker activates neurons to control a rhythmic behavior. *Curr Biol*. 23: 746–754.
25 McIntire SL, Jorgensen E, Kaplan J, Horvitz HR. 1993b. The GABAergic nervous system of *Caenorhabditis elegans*. *Nature*. 364:337–341.
26 Beg AA, Jorgensen EM. 2003. EXP-1 is an excitatory GABA-gated cation channel. *Nat Neurosci*. 6:1145–1152.
27 Miller AN, Long SB. 2012. Crystal structure of the human two-pore domain potassium channel K2P1. *Science*. 335:432–6.
28 Brohawn SG, Mármol JD, MacKinnon R. 2012. Crystal structure of the human K2P TRAAK, a lipid- and mechano-sensitive K^+ ion channel. *Science*. 335:436–441.
29 Natale AM, Deal PE, Minor DL Jr. 2021. Structural insights into the mechanisms and pharmacology of K_{2P} potassium channels. *J Mol Biol*. 433:166995.
30 Meng J, *et al.* 2024. A tonically active master neuron modulates mutually exclusive motor states at two timescales. *Sci Adv*. 10: eadk0002.
31 Lee J, Song HO, Jee C, Vanoaica L, Ahnn J. 2005. Calcineurin regulates enteric muscle contraction through EXP-1, excitatory GABA-gated channel, in *C. elegans*. *J Mol Biol*. 352:313–318.
32 Jin Y, Jorgensen E, Hartwieg E, Horvitz HR. 1999. The *Caenorhabditis elegans* gene *unc-25* encodes glutamic acid decarboxylase and is required for synaptic transmission but not synaptic development. *J Neurosci*. 19:539–548.
33 Li Y, *et al.* 2023. UBR-1 ubiquitin ligase regulates the balance between GABAergic and glutamatergic signaling. *EMBO Rep*. 24:e57014.
34 Brose N, Hofmann K, Hata Y, Sudhof TC. 1995. Mammalian homologues of *Caenorhabditis elegans unc-13* gene define novel family of C2-domain proteins. *J Biol Chem*. 270:25273–25280.
35 Gao S, Zhen M. 2011. Action potentials drive body wall muscle contractions in *Caenorhabditis elegans*. *Proc Natl Acad Sci USA*. 108:2557–2562.
36 Richmond JE, Jorgensen EM. 1999. One GABA and two acetylcholine receptors function at the *C. elegans* neuromuscular junction. *Nat Neurosci*. 2:791–797.
37 LeBoeuf B, Garcia LR. 2017. *Caenorhabditis elegans* male copulation circuitry incorporates sex-shared defecation components to promote intromission and sperm transfer. *G3 (Bethesda)*. 7: 647–662.
38 Jiang J, *et al.* 2022. *C. elegans* enteric motor neurons fire synchronized action potentials underlying the defecation motor program. *Nat Commun*. 13:2783.
39 Xie L, *et al.* 2013. NLF-1 delivers a sodium leak channel to regulate neuronal excitability and modulate rhythmic locomotion. *Neuron*. 77:1069–1082.
40 Wang H, Sieburth D. 2013. PKA controls calcium influx into motor neurons during a rhythmic behavior. *PLoS Genet*. 9:e1003831.
41 Johnstone DB, Wei A, Butler A, Salkoff L, Thomas JH. 1997. Behavioral defects in *C. elegans egl-36* mutants result from potassium channels shifted in voltage-dependence of activation. *Neuron*. 19:151–164.
42 Kunkel MT, Johnstone DB, Thomas JH, Salkoff L. 2000. Mutants of a temperature-sensitive two-P domain potassium channel. *J Neurosci*. 20:7517–7524.
43 de la Cruz IP, Ma L, Horvitz HR. 2014. The *Caenorhabditis elegans* iodotyrosine deiodinase ortholog SUP-18 functions through a conserved channel SC-box to regulate the muscle two-pore domain potassium channel SUP-9. *PLoS Genet*. 10: e1004175.
44 Kasap M, Weeks K, Aamodt EJ, Dwye DS. 2018. Gain-of-function mutations in a two-pore domain K^+ channel (*unc-58*) cause developmental, motor and feeding defects in *C. elegans* modified by temperature and a channel inhibitor, loratadine. *Curr Neurobiol*. 9:84–91.
45 Salkoff L, *et al.* 2005. *Potassium channels in C. elegans*. The C. elegans Research Community, WormBook. p. 1–15. doi:10.1895/wormbook.1.42.1. http://www.wormbook.org: WormBook.

46 Gottschling DC, Doring F, Luersen K. 2017. Locomotion behavior is affected by the GalphaS pathway and the two-pore-domain K^+ channel TWK-7 interacting in GABAergic motor neurons in *Caenorhabditis elegans*. *Genetics*. 206:283–297.
47 Luersen K, Gottschling DC, Doring F. 2016. Complex locomotion behavior changes are induced in *Caenorhabditis elegans* by the lack of the regulatory leak K^+ channel TWK-7. *Genetics*. 204: 683–701.
48 Zhou C, *et al*. 2022. Differential modulation of *C. elegans* motor behavior by NALCN and two-pore domain potassium channels. *PLoS Genet*. 18:e1010126.
49 Czirjak G, Enyedi P. 2002. Formation of functional heterodimers between the TASK-1 and TASK-3 two-pore domain potassium channel subunits. *J Biol Chem*. 277:5426–5432.
50 Beg AA, Ernstrom GG, Nix P, Davis MW, Jorgensen EM. 2008. Protons act as a transmitter for muscle contraction in *C. elegans*. *Cell*. 132:149–160.
51 Taylor SR, *et al*. 2021. Molecular topography of an entire nervous system. *Cell*. 184(16):4329–4347.
52 Liu C, Au JD, Zou HL, Cotten JF, Yost CS. 2004. Potent activation of the human tandem pore domain K channel TRESK with clinical concentrations of volatile anesthetics. *Anesth Analg*. 99:1715–1722.
53 Patel AJ, *et al*. 1999. Inhalational anesthetics activate two-pore-domain background K^+ channels. *Nat Neurosci*. 2:422–426.
54 Sirois JE, Lei Q, Talley EM, Lynch C 3rd, Bayliss DA. 2000. The TASK-1 two-pore domain K^+ channel is a molecular substrate for neuronal effects of inhalation anesthetics. *J Neurosci*. 20: 6347–6354.